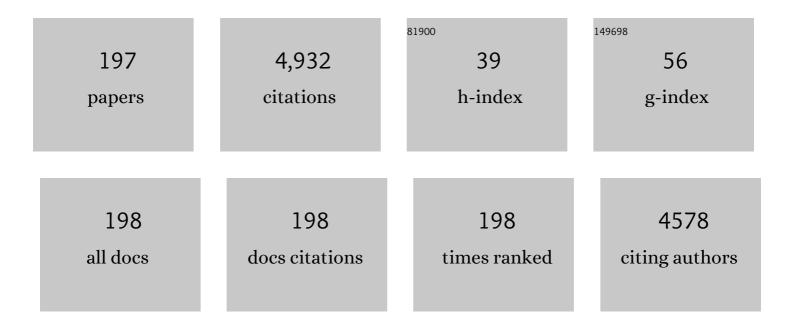
Ming-Yen Wey

List of Publications by Year in descending order

Source: https://exaly.com/author-pdf/8634022/publications.pdf Version: 2024-02-01



#	Article	IF	CITATIONS
1	Comparison of the characteristics of bottom and fly ashes generated from various incineration processes. Journal of Hazardous Materials, 2006, 138, 594-603.	12.4	138
2	The effect of particle size distribution on minimum fluidization velocity at high temperature. Powder Technology, 2002, 126, 297-301.	4.2	124
3	Hydrogen production by biomass gasification in a fluidized-bed reactor promoted by an Fe/CaO catalyst. International Journal of Hydrogen Energy, 2012, 37, 6511-6518.	7.1	113
4	Study of SO2 adsorption and thermal regeneration over activated carbon-supported copper oxide catalysts. Carbon, 2004, 42, 2269-2278.	10.3	111
5	Preparation and characterization of multi-walled carbon nanotube/PBNPI nanocomposite membrane for H2/CH4 separation. International Journal of Hydrogen Energy, 2009, 34, 8707-8715.	7.1	104
6	Catalytic removal of SO2, NO and HCl from incineration flue gas over activated carbon-supported metal oxides. Carbon, 2003, 41, 1079-1085.	10.3	98
7	Simultaneous removal of VOC and NO by activated carbon impregnated with transition metal catalysts in combustion flue gas. Fuel Processing Technology, 2007, 88, 557-567.	7.2	97
8	Carbon materials as catalyst supports for SO2 oxidation: catalytic activity of CuO–AC. Carbon, 2003, 41, 139-149.	10.3	93
9	Thermal treatment of the fly ash from municipal solid waste incinerator with rotary kiln. Journal of Hazardous Materials, 2006, 137, 981-989.	12.4	86
10	A comparison of carbon/nanotube molecular sieve membranes with polymer blend carbon molecular sieve membranes for the gas permeation application. Microporous and Mesoporous Materials, 2008, 113, 499-510.	4.4	83
11	Fabrication and characterization of PPO/PVP blend carbon molecular sieve membranes for H2/N2 and H2/CH4 separation. Journal of Membrane Science, 2011, 372, 387-395.	8.2	80
12	Evaluation of the distribution patterns of Pb, Cu and Cd from MSWI fly ash during thermal treatment by sequential extraction procedure. Journal of Hazardous Materials, 2009, 162, 1000-1006.	12.4	78
13	Photocatalytic properties of redox-treated Pt/TiO2 photocatalysts for H2 production from an aqueous methanol solution. International Journal of Hydrogen Energy, 2010, 35, 7699-7705.	7.1	78
14	The properties and filtration efficiency of activated carbon polymer composite membranes for the removal of humic acid. Desalination, 2013, 313, 166-175.	8.2	73
15	Effects of Nickel Species on Ni/Al ₂ O ₃ Catalysts in Carbon Nanotube and Hydrogen Production by Waste Plastic Gasification: Bench- and Pilot-Scale Tests. Energy & Fuels, 2015, 29, 8178-8187.	5.1	73
16	The effect of mineral compositions of waste and operating conditions on particle agglomeration/defluidization during incineration. Fuel, 2004, 83, 2335-2343.	6.4	68
17	Effects of acid treatments of activated carbon on its physiochemical structure as a support for copper oxide in DeSO2 reaction catalysts. Chemosphere, 2006, 62, 756-766.	8.2	63
18	Preparation and characterization of carbon molecular sieve membranes for gas separation—the effect of incorporated multi-wall carbon nanotubes. Desalination, 2009, 240, 40-45.	8.2	58

Ming-Yen Wey

#	Article	IF	CITATIONS
19	Effect of particle agglomeration on heavy metals adsorption by Al- and Ca-based sorbents during fluidized bed incineration. Fuel Processing Technology, 2011, 92, 2089-2098.	7.2	58
20	Fabrication and characterization of poly(phenylene oxide)/SBA-15/carbon molecule sieve multilayer mixed matrix membrane for gas separation. International Journal of Hydrogen Energy, 2010, 35, 6971-6983.	7.1	57
21	Co-production of carbon nanotubes and hydrogen from waste plastic gasification in a two-stage fluidized catalytic bed. Renewable Energy, 2020, 159, 10-22.	8.9	57
22	Application of polyol process to prepare AC-supported nanocatalyst for VOC oxidation. Applied Catalysis A: General, 2007, 325, 163-174.	4.3	54
23	The performance of CNT as catalyst support on CO oxidation at low temperature. Fuel, 2007, 86, 1153-1161.	6.4	51
24	Inhibition and promotion: The effect of earth alkali metals and operating temperature on particle agglomeration/defluidization during incineration in fluidized bed. Powder Technology, 2009, 189, 57-63.	4.2	51
25	Formations and controls of HCl and PAHs by different additives during waste incineration. Fuel, 2006, 85, 755-763.	6.4	48
26	Photocatalytic conversion of simulated EDTA wastewater to hydrogen by pH-resistant Pt/TiO2–activated carbon photocatalysts. Renewable Energy, 2015, 75, 266-271.	8.9	48
27	Adsorption Mechanism of Heavy Metals on Sorbents during Incineration. Journal of Environmental Engineering, ASCE, 2001, 127, 63-69.	1.4	47
28	Influence of support structure on the permeation behavior of polyetherimide-derived carbon molecular sieve composite membrane. Journal of Membrane Science, 2012, 405-406, 250-260.	8.2	46
29	Effect of dry/wet-phase inversion method on fabricating polyetherimide-derived CMS membrane for H2/N2 separation. International Journal of Hydrogen Energy, 2010, 35, 1650-1658.	7.1	44
30	Hydrogen production through methanol steam reforming: Effect of synthesis parameters on Ni–Cu/CaO–SiO 2 catalysts activity. International Journal of Hydrogen Energy, 2014, 39, 19494-19501.	7.1	44
31	Reuse of bottom ash and fly ash from mechanical-bed and fluidized-bed municipal incinerators in manufacturing lightweight aggregates. Ceramics International, 2018, 44, 12691-12696.	4.8	44
32	The behavior of heavy metal Cr,Pb and Cd during waste incineration in fluidized bed under various chlorine additives Journal of Chemical Engineering of Japan, 1996, 29, 494-500.	0.6	42
33	Effect of SBA-15 texture on the gas separation characteristics of SBA-15/polymer multilayer mixed matrix membrane. Journal of Membrane Science, 2011, 369, 550-559.	8.2	42
34	NO removal by activated carbon-supported copper catalysts prepared by impregnation, polyol, and microwave heated polyol processes. Applied Catalysis A: General, 2011, 397, 234-240.	4.3	42
35	Effects of Temperature and Equivalence Ratio on Carbon Nanotubes and Hydrogen Production from Waste Plastic Gasification in Fluidized Bed. Energy & Fuels, 2018, 32, 5462-5470.	5.1	42
36	Theoretical and Experimental Study of Metal Capture during Incineration Process. Journal of Environmental Engineering, ASCE, 1997, 123, 1100-1106.	1.4	41

#	Article	IF	CITATIONS
37	The prospect and development of incinerators for municipal solid waste treatment and characteristics of their pollutants in Taiwan. Applied Thermal Engineering, 2008, 28, 2305-2314.	6.0	41
38	Preparation of PPO-silica mixed matrix membranes by in-situ sol–gel method for H2/CO2 separation. International Journal of Hydrogen Energy, 2014, 39, 17178-17190.	7.1	41
39	The influence of heavy metals on the formation of organics and HCl during incinerating of PVC-containing waste. Journal of Hazardous Materials, 1998, 60, 259-270.	12.4	40
40	Two-stage simulation of the major heavy-metal species under various incineration conditions. Environment International, 1998, 24, 451-466.	10.0	39
41	Simultaneous treatment of organic compounds, CO, and NOx in the incineration flue gas by three-way catalyst. Applied Catalysis B: Environmental, 2004, 48, 25-35.	20.2	37
42	Cadmium Stabilization Efficiency and Leachability by CdAl ₄ O ₇ Monoclinic Structure. Environmental Science & Technology, 2015, 49, 14452-14459.	10.0	37
43	The size, shape, and dispersion of active sites on AC-supported copper nanocatalysts with polyol process: The effect of precursors. Applied Catalysis A: General, 2008, 344, 36-44.	4.3	36
44	Enhanced optical and electronic properties of a solar light-responsive photocatalyst for efficient hydrogen evolution by SrTiO3/TiO2 nanotube combination. Solar Energy, 2016, 134, 52-63.	6.1	35
45	Preparation and characterization of PPSU/PBNPI blend membrane for hydrogen separation. International Journal of Hydrogen Energy, 2008, 33, 4178-4182.	7.1	34
46	Catalytic upgrading of syngas from fluidized bed air gasification of sawdust. Bioresource Technology, 2012, 110, 670-675.	9.6	34
47	The density and crystallinity properties of PPO-silica mixed-matrix membranes produced via the in situ sol-gel method for H2/CO2 separation. II: Effect of thermal annealing treatment. Chemical Engineering Research and Design, 2015, 104, 319-332.	5.6	33
48	The influence of heavy metals on partitioning of PAHs during incineration. Journal of Hazardous Materials, 2000, 77, 77-87.	12.4	32
49	Control of acid gases using a fluidized bed adsorber. Journal of Hazardous Materials, 2003, 101, 259-272.	12.4	32
50	Al2O3-supported Cu–Co bimetallic catalysts prepared with polyol process for removal of BTEX and PAH in the incineration flue gas. Fuel, 2009, 88, 340-347.	6.4	32
51	Properties and H2 production ability of Pt photodeposited on the anatase phase transition of nitrogen-doped titanium dioxide. International Journal of Hydrogen Energy, 2011, 36, 9479-9486.	7.1	32
52	Improving the mechanical strength and gas separation performance of CMS membranes by simply sintering treatment of α-Al2O3 support. Journal of Membrane Science, 2014, 453, 603-613.	8.2	32
53	The Autothermal Pyrolysis of Waste Tires. Journal of the Air and Waste Management Association, 1995, 45, 855-863.	1.9	31
54	Influence of hydrodynamic parameters on particle attrition during fluidization at high temperature. Korean Journal of Chemical Engineering, 2005, 22, 154-160.	2.7	31

#	Article	IF	CITATIONS
55	Ni/SiO 2 core–shell catalysts for catalytic hydrogen production from waste plastics-derived syngas. International Journal of Hydrogen Energy, 2017, 42, 11239-11251.	7.1	31
56	Thermal degradation of waste plastics in a two-stage pyrolysis-catalysis reactor over core-shell type catalyst. Journal of Analytical and Applied Pyrolysis, 2019, 142, 104641.	5.5	31
57	Feasibility of using waste polystyrene as a membrane material for gas separation. Chemical Engineering Research and Design, 2016, 111, 204-217.	5.6	30
58	Creation of tiny defects in ZIF-8 by thermal annealing to improve the CO2/N2 separation of mixed matrix membranes. Journal of Membrane Science, 2019, 572, 410-418.	8.2	30
59	The effect of ash and filter media characteristics on particle filtration efficiency in fluidized bed. Journal of Hazardous Materials, 2005, 121, 175-181.	12.4	29
60	Thermal treatment of soil co-contaminated with lube oil and heavy metals in a low-temperature two-stage fluidized bed incinerator. Applied Thermal Engineering, 2016, 93, 131-138.	6.0	29
61	Synthesis of solar-light responsive Pt/g-C3N4/SrTiO3 composite for improved hydrogen production: Investigation of Pt/g-C3N4/SrTiO3 synthetic sequences. International Journal of Hydrogen Energy, 2019, 44, 21413-21423.	7.1	29
62	Emission of carbon dioxide in municipal solid waste incineration in Taiwan: A comparison with thermal power plants. International Journal of Greenhouse Gas Control, 2011, 5, 889-898.	4.6	28
63	Emission characteristics of organic and heavy metal pollutants in fluidized bed incineration during the agglomeration/defluidization process. Combustion and Flame, 2005, 143, 139-149.	5.2	27
64	Carbon nanotube and hydrogen production from waste plastic gasification over Ni/Al–SBA-15 catalysts: effect of aluminum content. RSC Advances, 2016, 6, 40731-40740.	3.6	27
65	Effect of MFI zeolite intermediate layers on gas separation performance of carbon molecular sieve (CMS) membranes. Journal of Membrane Science, 2013, 446, 220-229.	8.2	26
66	The comparison between the polyol process and the impregnation method for the preparation of CNT-supported nanoscale Cu catalyst. Chemical Engineering Journal, 2009, 145, 461-467.	12.7	25
67	Facile approach for Z-scheme type Pt/g-C3N4/SrTiO3 heterojunction semiconductor synthesis via low-temperature process for simultaneous dyes degradation and hydrogen production. International Journal of Hydrogen Energy, 2020, 45, 13330-13339.	7.1	25
68	Stability of heavy metals in bottom ash and fly ash under various incinerating conditions. Journal of Hazardous Materials, 1998, 57, 145-154.	12.4	24
69	The Relationship between the Quantity of Heavy Metal and PAHs in Fly Ash. Journal of the Air and Waste Management Association, 1998, 48, 750-756.	1.9	24
70	Effects of high temperature and combustion on fluidized material attrition in a fluidized bed. Korean Journal of Chemical Engineering, 2003, 20, 1123-1130.	2.7	24
71	Design of a Pt/TiO2–xNx/SrTiO3 triplejunction for effective photocatalytic H2 production under solar light irradiation. Chemical Engineering Journal, 2013, 223, 854-859.	12.7	24
72	A novel technique using reclaimed tire rubber for gas separation membranes. Journal of Membrane Science, 2016, 520, 314-325.	8.2	24

#	Article	IF	CITATIONS
73	Reuse of reclaimed tire rubber for gas-separation membranes prepared by hot-pressing. Journal of Cleaner Production, 2019, 237, 117739.	9.3	24
74	Control of Incinerator Organics by Fluidized Bed Activated Carbon Adsorber. Journal of Environmental Engineering, ASCE, 2000, 126, 985-992.	1.4	23
75	Emission of Pb and PAHs from thermally co-treated MSWI fly ash and bottom ash process. Journal of Hazardous Materials, 2008, 150, 27-36.	12.4	23
76	An efficient composite growing N-doped TiO2 on multi-walled carbon nanotubes through sol–gel process. Journal of Nanoparticle Research, 2010, 12, 2503-2510.	1.9	23
77	Design of a solar light-responsive metal oxide/CdS/SrTiO 3 catalyst with enhanced charge separation for hydrogen evolution. Solar Energy, 2017, 147, 240-247.	6.1	23
78	Comparison of visible-light-driven routes of anion-doped TiO2 and composite photocatalyst. Journal of the Ceramic Society of Japan, 2009, 117, 753-758.	1.1	22
79	Catalytic treating of gas pollutants over cobalt catalyst supported on porous carbons derived from rice husk and carbon nanotube. Applied Catalysis B: Environmental, 2009, 90, 652-661.	20.2	21
80	Evaluation of SO2 oxidation and fly ash filtration by an activated carbon fluidized-bed reactor: The effects of acid modification, copper addition and operating condition. Fuel, 2010, 89, 732-742.	6.4	21
81	Catalytic removal of NO and PAHs over AC-supported catalysts from incineration flue gas: Bench-scale and pilot-plant tests. Chemical Engineering Journal, 2011, 169, 135-143.	12.7	21
82	Structure-controlled mesoporous SBA-15-derived mixed matrix membranes for H2 purification and CO2 capture. International Journal of Hydrogen Energy, 2017, 42, 11379-11391.	7.1	21
83	Filtration of nano-particles by a gas–solid fluidized bed. Journal of Hazardous Materials, 2007, 147, 618-624.	12.4	20
84	Effects of sodium modification, different reductants and SO2 on NO reduction by Rh/Al2O3 catalysts at excess O2 conditions. Journal of Hazardous Materials, 2008, 156, 348-355.	12.4	20
85	The effect of aluminum inhibition on the defluidization behavior and generation of pollutants in fluidized bed incineration. Fuel Processing Technology, 2008, 89, 1227-1236.	7.2	20
86	The different properties of lightweight aggregates with the fly ashes of fluidized-bed and mechanical incinerators. Construction and Building Materials, 2015, 101, 380-388.	7.2	20
87	Hydrogen promotion by Co/SiO2@HZSM-5 core-shell catalyst for syngas from plastic waste gasification: The combination of functional materials. International Journal of Hydrogen Energy, 2019, 44, 13480-13489.	7.1	20
88	Interfacial interaction between CMS layer and substrate: Critical factors affecting membrane microstructure and H2 and CO2 separation performance from CH4. Journal of Membrane Science, 2019, 580, 49-61.	8.2	20
89	Activity and characterization of Rh/Al2O3 and Rh–Na/Al2O3 catalysts for the SCR of NO with CO in the presence of SO2 and HCl. Fuel, 2010, 89, 1919-1927.	6.4	18
90	Effect of alkali concentrations and operating conditions on agglomeration/defluidization behavior during fluidized bed air gasification. Powder Technology, 2011, 214, 443-446.	4.2	18

#	Article	IF	CITATIONS
91	CuO/CeO2 catalysts prepared with different cerium supports for CO oxidation at low temperature. Materials Chemistry and Physics, 2013, 141, 512-518.	4.0	18
92	Prediction of defluidization time of alkali composition at various operating conditions during incineration. Powder Technology, 2006, 161, 150-157.	4.2	17
93	Collection of SiO2, Al2O3 and Fe2O3 particles using a gas-solid fluidized bed filter. Journal of Hazardous Materials, 2009, 171, 102-110.	12.4	17
94	Design of catalysts comprising a nickel core and ceria shell for hydrogen production from plastic waste gasification: an integrated test for anti-coking and catalytic performance. Catalysis Science and Technology, 2020, 10, 3975-3984.	4.1	17
95	Synthesis of carbon nanotubes with controllable diameter by chemical vapor deposition of methane using Fe@Al2O3 core–shell nanocomposites. Chemical Engineering Science, 2020, 217, 115541.	3.8	17
96	Solvent effects on diffusion channel construction of organosilica membrane with excellent CO2 separation properties. Journal of Membrane Science, 2021, 618, 118758.	8.2	17
97	Characterizing PAH emission concentrations in ambient air during a large-scale joss paper open-burning event. Journal of Hazardous Materials, 2008, 156, 223-229.	12.4	16
98	Enhancing the CO2 plasticization resistance of PS mixed-matrix membrane by blunt zeolitic imidazolate framework. Journal of CO2 Utilization, 2018, 25, 79-88.	6.8	16
99	Evaluating the potential of CNT-supported Co catalyst used for gas pollution removal in the incineration flue gas. Journal of Environmental Management, 2009, 90, 1884-1892.	7.8	15
100	Effect of agglomeration/defluidization on hydrogen generation during fluidized bed air gasification of modified biomass. International Journal of Hydrogen Energy, 2012, 37, 1409-1417.	7.1	15
101	Facile synthesis of CO2-selective membrane derived from butyl reclaimed rubber (BRR) for efficient CO2 separation. Journal of CO2 Utilization, 2018, 25, 226-234.	6.8	15
102	Core-shell design and well-dispersed Pd particles for three-way catalysis: Effect of halloysite nanotubes functionalized with Schiff base. Science of the Total Environment, 2019, 675, 397-407.	8.0	15
103	Thin carbon hollow fiber membrane with Knudsen diffusion for hydrogen/alkane separation: Effects of hollow fiber module design and gas flow mode. International Journal of Hydrogen Energy, 2020, 45, 7290-7302.	7.1	15
104	Design of a thermally resistant core@shell/halloysite catalyst with optimized structure and surface properties for a Pd-only three-way catalyst. Applied Catalysis A: General, 2020, 602, 117732.	4.3	15
105	Filtration of Fly Ash Using a Fluidized-Bed Filter. Journal of the Air and Waste Management Association, 2005, 55, 181-193.	1.9	14
106	Filtration of fly ash using fluidized bed at 300–500°C. Fuel, 2007, 86, 161-168.	6.4	14
107	Effects of the ratio of Cu/Co and metal precursors on the catalytic activity over Cu-Co/Al2O3 prepared using the polyol process. Materials Science and Engineering B: Solid-State Materials for Advanced Technology, 2009, 157, 105-112.	3.5	14
108	Mechanisms of particle agglomeration and inhibition approach in the existence of heavy metals during fluidized bed incineration. Chemical Engineering Science, 2010, 65, 4955-4966.	3.8	14

#	Article	IF	CITATIONS
109	Study on Pb and PAHs Emission Levels of Heavy Metals- and PAHs-Contaminated Soil during Thermal Treatment Process. Journal of Environmental Engineering, ASCE, 2010, 136, 112-118.	1.4	14
110	Insights into the Role of Polymer Conformation on the Cutoff Size of Carbon Molecular Sieving Membranes for Hydrogen Separation and Its Novel Pore Size Detection Technology. ACS Applied Materials & Interfaces, 2021, 13, 5165-5175.	8.0	14
111	Mass and Elemental Size Distribution of Chromium, Lead and Cadmium under Various Incineration Conditions Journal of Chemical Engineering of Japan, 1998, 31, 506-517.	0.6	14
112	Catalytic activity of copper-supported catalyst for NO reduction in the presence of oxygen: Fitting of calcination temperature and copper loading. Materials Science and Engineering B: Solid-State Materials for Advanced Technology, 2010, 175, 100-107.	3.5	13
113	Removals of fly ash and NO in a fluidized-bed reactor with CuO/activated carbon catalysts. Journal of Hazardous Materials, 2011, 187, 190-198.	12.4	13
114	Development of a low-temperature two-stage fluidized bed incinerator for controlling heavy-metal emission in flue gases. Applied Thermal Engineering, 2014, 62, 706-713.	6.0	13
115	Sintering-resistant, highly thermally stable and well-dispersed Pd@CeO2/halloysite as an advanced three-way catalyst. Science of the Total Environment, 2020, 707, 136137.	8.0	13
116	Dynamic purification of coal ash by a gas–solid fluidized bed. Chemosphere, 2005, 60, 1341-1348.	8.2	12
117	Catalytic removal of NO in waste incineration processes over Rh/Al2O3 and Rh–Na/Al2O3: Effects of particulates, heavy metals, SO2 and HCl. Fuel Processing Technology, 2009, 90, 576-582.	7.2	12
118	Study of the activity and backscattered electron image of Pt/CNTs prepared by the polyol process for flue gas purification. Applied Catalysis A: General, 2009, 354, 57-62.	4.3	12
119	Study of SBA-15 supported catalysts for toluene and NO removal: the effect of promoters (Co, Ni, Mn,) Tj ETQq1	1 0.78431 1.7	4.rgBT /Over
120	Development of CMS/Al2O3-supported PPO composite membrane for hydrogen separation. International Journal of Hydrogen Energy, 2013, 38, 3092-3104.	7.1	12
121	Woody waste air gasification in fluidized bed with Ca- and Mg-modified bed materials and additives. Applied Thermal Engineering, 2013, 53, 42-48.	6.0	12
122	Copper catalysts prepared via microwave-heated polyol process for preferential oxidation of CO in H2-rich streams. International Journal of Hydrogen Energy, 2013, 38, 100-108.	7.1	12
123	Effects of membrane compositions and operating conditions on the filtration and backwashing performance of the activated carbon polymer composite membranes. Desalination, 2014, 352, 181-189.	8.2	12
124	A carbon gutter layer-modified α-Al2O3 substrate for PPO membrane fabrication and CO2 separation. Journal of Membrane Science, 2014, 454, 51-61.	8.2	12
125	The influence of matrix structure and thermal annealing-hydrophobic layer on the performance and durability of carbon molecular sieving membrane during physical aging. Journal of Membrane Science, 2015, 495, 294-304.	8.2	12
126	Development of physicochemically stable Z-scheme MIL-88A/g-C3N4 heterojunction photocatalyst with excellent charge transfer for improving acid red 1 dye decomposition efficiency. Applied Surface Science, 2022, 590, 152954.	6.1	12

#	Article	IF	CITATIONS
127	Effects of particulates, heavy metals and acid gas on the removals of NO and PAHs by V2O5–WO3 catalysts in waste incineration system. Journal of Hazardous Materials, 2009, 170, 239-246.	12.4	11
128	Gaseous organic emissions during air gasification of woody waste: effect of bed agglomeration/defluidization. Fuel Processing Technology, 2014, 128, 104-110.	7.2	11
129	Excellent dispersion and charge separation of SrTiO3-TiO2 nanotube derived from a two-step hydrothermal process for facilitating hydrogen evolution under sunlight irradiation. Solar Energy, 2018, 159, 751-759.	6.1	11
130	Catalytic Methane Decomposition to Hydrogen over a Surfaceâ€Protected Core‧hell Ni@SiO ₂ Catalyst. Chemical Engineering and Technology, 2018, 41, 1448-1456.	1.5	11
131	Recycling waste plastics as hollow fiber substrates to improve the anti-wettability of supported ionic liquid membranes for CO2 separation. Journal of Cleaner Production, 2020, 276, 124194.	9.3	11
132	Influence of Operating Conditions on the Formation of Heavy Metal Compounds During Incineration. Journal of the Air and Waste Management Association, 1999, 49, 444-453.	1.9	10
133	The Utilization of Catalyst Sorbent in Scrubbing Acid Gases from Incineration Flue Gas. Journal of the Air and Waste Management Association, 2002, 52, 449-458.	1.9	10
134	Relationship between pressure fluctuations and generation of organic pollutants with different particle size distributions in a fluidized bed incinerator. Chemosphere, 2004, 56, 911-922.	8.2	10
135	Sustainable hydrogen production from electroplating wastewater over a solar light responsive photocatalyst. RSC Advances, 2016, 6, 71273-71281.	3.6	10
136	Effect of copolymer microphase-separated structures on the gas separation performance and aging properties of SBC-derived membranes. Journal of Membrane Science, 2017, 529, 63-71.	8.2	10
137	Fabrication of waterproof gas separation membrane from plastic waste for CO2 separation. Environmental Research, 2021, 195, 110760.	7.5	10
138	High loading and high-selectivity H2 purification using SBC@ZIF based thin film composite hollow fiber membranes. Journal of Membrane Science, 2021, 626, 119191.	8.2	10
139	Simulation of agglomeration/defluidization inhibition process in aluminum–sodium system by experimental and thermodynamic approaches. Powder Technology, 2012, 224, 395-403.	4.2	9
140	Influence of thermal treatment atmosphere on photogenerated charge separation of Pt/N–TiO2/SrTiO3 for efficient hydrogen evolution. Journal of Materials Science, 2015, 50, 5873-5885.	3.7	9
141	Study of the low-temperature two-stage fluidized bed incineration: Influence of the second-stage sand bed operating conditions on pollutant emission. Applied Thermal Engineering, 2015, 75, 592-599.	6.0	9
142	Effect of co-contaminated soil mixtures as fixed/fluidized bed media on pollutants emission under thermal treatment. International Journal of Environmental Science and Technology, 2016, 13, 519-528.	3.5	9
143	Enrichment of Hydrogen Production from Biomassâ€Gasificationâ€Derived Syngas over Spinelâ€Type Aluminateâ€Supported Nickel Catalysts. Energy Technology, 2018, 6, 318-325.	3.8	9
144	Positive effects of a halloysite-supported Cu/Co catalyst fabricated by a urea-driven deposition precipitation method on the CO-SCR reaction and SO ₂ poisoning. Catalysis Science and Technology, 2021, 11, 3456-3465.	4.1	9

#	Article	IF	CITATIONS
145	Impacts of Green Synthesis Process on Asymmetric Hybrid PDMS Membrane for Efficient CO2/N2 Separation. Membranes, 2021, 11, 59.	3.0	9
146	Highly abrasion and coking-resistance core-shell catalyst for hydrogen-rich syngas production from waste plastics in a two-staged fluidized bed reactor. Applied Catalysis A: General, 2021, 612, 117989.	4.3	9
147	Excellent dispersion of solar light responsive photocatalyst in the different polymer films for easy recycling and sustainable hydrogen production. Solar Energy, 2022, 231, 949-957.	6.1	9
148	Thermal Treatment for Incinerator Ash: Evaporation and Leaching Rates of Metals. Journal of Environmental Engineering, ASCE, 2003, 129, 258-266.	1.4	8
149	Effect of concentration of bed materials on combustion efficiency during incineration. Energy, 2004, 29, 125-136.	8.8	8
150	Partitioning and Emission Characteristics of Pb and Organics during Fluidized Bed Thermal Treatment of Municipal Solid Waste Incineration (MSWI) Fly Ash. Energy & Fuels, 2008, 22, 3789-3797.	5.1	8
151	Effects of Agglomeration Processes on the Emission Characteristics of Heavy Metals under Different Waste Compositions and the Addition of Al and Ca Inhibitors in Fluidized Bed Incineration. Energy & Fuels, 2009, 23, 4325-4336.	5.1	8
152	Effects of microwave power and polyvinyl pyrrolidone on microwave polyol process of carbon-supported Cu catalysts for CO oxidation. Materials Science and Engineering B: Solid-State Materials for Advanced Technology, 2011, 176, 745-749.	3.5	8
153	Characterization of N-doped TiO2 nanoparticles supported on SrTiO3 via a sol–gel process. Journal of Nanoparticle Research, 2014, 16, 1.	1.9	8
154	Tuning thermal expansion behavior and surface roughness of tubular Al2O3 substrates for fabricating high-performance carbon molecular sieving membranes for H2 separation. International Journal of Hydrogen Energy, 2019, 44, 24746-24758.	7.1	8
155	Effect of Preparation Solvent and Calcination Atmosphere on Ni@SiO 2 Catalyst for Simultaneous Production of Hydrogen and Carbon Nanotubes from Simulated Plastic Waste Syngas. Energy Technology, 2019, 7, 1800586.	3.8	8
156	The Viable Fabrication of Gas Separation Membrane Used by Reclaimed Rubber from Waste Tires. Polymers, 2020, 12, 2540.	4.5	8
157	Catalytic Oxidation of Organic Compounds in Incineration Flue Gas by a Commercial Palladium Catalyst. Journal of the Air and Waste Management Association, 2002, 52, 198-207.	1.9	7
158	EMISSION CHARACTERISTICS OF CHLOROBENZENES, CHLOROPHENOLS AND DIOXINS DURING WASTE INCINERATION WITH DIFFERENT ADDITIVES. Combustion Science and Technology, 2007, 179, 1039-1058.	2.3	7
159	The activity of Rh/Al2O3 and Rh–Na/Al2O3 catalysts for PAHs removal in the waste incineration processes: Effects of particulates, heavy metals, and acid gases. Fuel, 2009, 88, 1563-1571.	6.4	7
160	Effects of oxygen and hydrogen chloride on NO removal efficiency by Rh/Al2O3 and Rh–Na/Al2O3 catalysts. Applied Catalysis A: General, 2009, 359, 88-95.	4.3	7
161	Removal of NO and fly ash over a carbon supported catalyst: Effects of fly ash concentration and operating time. Powder Technology, 2013, 239, 239-247.	4.2	7
162	Green Route for Hydrogen Evolution from Real Electroplating Waste Liquids Induced by a Solar Light Responsive Photocatalyst. ACS Sustainable Chemistry and Engineering, 2017, 5, 2146-2153.	6.7	7

#	Article	IF	CITATIONS
163	PVA/Pt/N-TiO2/SrTiO3 porous films with adjustable pore size for hydrogen production under simulated sunlight. Journal of Colloid and Interface Science, 2020, 573, 158-164.	9.4	7
164	Synthesis of Ni@Al2O3 nanocomposite with superior activity and stability for hydrogen production from plastic-derived syngas by CO2-sorption-enhanced reforming. International Journal of Hydrogen Energy, 2021, 46, 39728-39735.	7.1	7
165	Dual immobilization of Pd Cu nanoparticles on halloysite nanotubes by CTAB and PVP for automobile exhaust elimination. Applied Clay Science, 2021, 214, 106299.	5.2	7
166	The Effects of Chloride Additives on Adsorption of Heavy Metals during Incineration. Journal of the Air and Waste Management Association, 1999, 49, 1116-1120.	1.9	6
167	Oxidation of organic pollutants in incineration flue gas by a fluidized palladium catalyst. Combustion Science and Technology, 2003, 175, 1211-1236.	2.3	6
168	Removal the Coal Ash, NO, and SO ₂ Simultaneously by the Fluidized-Bed Catalyst Reactor. Energy & Fuels, 2010, 24, 1711-1719.	5.1	6
169	Characterization and photoactivity of Pt/N-doped TiO2 synthesized through a sol–gel process at room temperature. Journal of Nanoparticle Research, 2015, 17, 1.	1.9	6
170	Uniformity control and ultraâ€micropore development of tubular carbon membrane for light gas separation. AICHE Journal, 2020, 66, e16226.	3.6	6
171	In situ phase transformation of polytypic zinc-blende/wurtzite copper indium sulfide via a facile polyol method to boost visible-light photocatalytic performance. Chemosphere, 2021, 277, 130348.	8.2	6
172	The Major Species of Heavy Metal Aerosol Resulting from Water Cooling Systems and Spray Dryer Systems during Incineration Processes. Journal of the Air and Waste Management Association, 1998, 48, 1069-1076.	1.9	5
173	The Capture of Heavy Metals from Incineration Using a Spray Dryer Integrated with a Fabric Filter Using Various Additives. Journal of the Air and Waste Management Association, 2001, 51, 983-991.	1.9	5
174	Effects of Na, Cu, Ni and Co Modifications on the Activity and Characteristics of Rh/Al2O3 Catalysts for NO Reduction. Catalysis Letters, 2008, 126, 207-211.	2.6	5
175	Determination of the Pb, Cr, and Cd distribution patterns with various chlorine additives in the bottom ashes of a low-temperature two-stage fluidized bed incinerator by chemical sequential extraction. Journal of Hazardous Materials, 2015, 295, 86-96.	12.4	5
176	Determination of Emission Characteristics during Thermal Treatment of Lube Oil and Heavy Metal Co-Contaminated Soil by Fluidized Bed Combustion. Journal of Environmental Engineering, ASCE, 2015, 141, .	1.4	5
177	Effect of polystyrene characteristic on photocatalytic hydrogen production by porous polystyrene photocatalyst film under simulated solar light irradiation. International Journal of Hydrogen Energy, 2021, 46, 11597-11606.	7.1	5
178	Effect of heat diffusivity for driving chain stitching of dual-type hybrid organosilica-derived membranes. Separation and Purification Technology, 2022, 290, 120848.	7.9	5
179	Effects of metal precursor in the sol–gel synthesis on the physicochemical properties of Pd/Al2O3–CeO2 catalyst: CO oxidation. Journal of Non-Crystalline Solids, 2006, 352, 2166-2172.	3.1	4
180	Photocatalytic conversion of ethylenediaminetetraacetic acid dissolved in real electroplating wastewater to hydrogen in a solar light-responsive system. Water Science and Technology, 2018, 77, 2851-2857.	2.5	4

#	Article	IF	CITATIONS
181	Highly Permeable Mixed Matrix Hollow Fiber Membrane as a Latent Route for Hydrogen Purification from Hydrocarbons/Carbon Dioxide. Membranes, 2021, 11, 865.	3.0	4
182	Effects of crosslinking modification on the O ₂ /N ₂ separation characteristics of poly(phenyl sulfone)/poly(bisphenol Aâ€ <i>co</i> â€4â€nitrophthalic) Tj ETQq0 0 0 rgBT /Overlock 10 Tf 50 70)2 Td (anh 2.6	ydŗideâ€∢i>c
	116, 1254-1263.		
183	Effects of H2O and Particles on the Simultaneous Removal of SO2 and Fly Ash Using a Fluidized-Bed Sorbent/Catalyst Reactor. Industrial & Engineering Chemistry Research, 2009, 48, 10541-10550.	3.7	3
184	Effect of Cu species on leaching behavior of simulated copper sludge after thermal treatment: ESCA analysis. Journal of Hazardous Materials, 2010, 179, 1106-1110.	12.4	3
185	Copper emission during thermal treatment of simulated copper sludge. Environmental Technology (United Kingdom), 2012, 33, 17-25.	2.2	3
186	The influences of microwave irradiation and polyol precursor pH on Cu/AC catalyst and its CO oxidation performance. Journal of Nanoparticle Research, 2012, 14, 1.	1.9	3
187	Acceleration of acid red 1 dye decolorization efficiency by adding methanol with simultaneous hydrogen production. International Journal of Environmental Science and Technology, 2019, 16, 8355-8362.	3.5	3
188	Photo-induced poly(styrene-[C1mim][Tf2N])-supported hollow fiber ionic liquid membranes to enhance CO2 separation. Journal of CO2 Utilization, 2022, 56, 101871.	6.8	3
189	Improving the Activity of Rh/Al2O3 Catalyst for NO Reduction by Na Addition in the Presences of H2O and O2. Catalysis Letters, 2009, 130, 517-524.	2.6	2
190	Enhanced O <inf>2</inf> /N <inf>2</inf> separation performance of poly(phenylene) Tj ETQq0 2010, , .	0 0 0 rgBT	/Overlock 10 2
191	Effect of operating conditions on emission concentration of PAHs during fluidized bed air gasification of biomass. , 2010, , .		2
192	Evaluating the Relationships between Pb Species and Leaching Properties in Simulated MSWI Fly Ash with Thermal Treatment by ESCA. Journal of Environmental Engineering, ASCE, 2012, 138, 632-636.	1.4	2
193	The Competitive Adsorption of Heavy Metals under Various Incineration Conditions Journal of Chemical Engineering of Japan, 2003, 36, 243-249.	0.6	2
194	Estimating the feasibility of raw carbon nanotubes used as catalyst for CO oxidation. , 2010, , .		0
195	An effective method for controlling the nanoparticle size of anatase TiO <inf>2</inf> . , 2010, , .		0
196	Filtration of nanoparticles by a fluidized-bed adsorption reactor during toluene adsorption. , 2010, , .		0
197	Carbon membrane for the application in gas separation: recent development and prospects. , 2022, , 177-214.		0